

Water Vapour Climate Change Initiative (WV_cci) - CCI+ Phase 1



ATBD Part 3 - Merged CDR-3 and CDR-4 products

Ref: D2.2

Date: 7 June 2022

Issue: 2.0

For: ESA / ECSAT

Ref: CCIWV.REP.022



Science & Technology Facilities Council
Rutherford Appleton Laboratory

Università deVigo

This Page is Intentionally Blank

Project : **Water Vapour Climate Change Initiative (WV_cci) - CCI+ Phase 1**

Document Title: **ATBD Part 3 - Merged CDR-3 and CDR-4 products**

Reference : **D2.2**

Issued : **07 June 2022**

Issue : **2.0**

Client: **ESA / ECSAT**

Author(s) : **Michaela Hegglin and Hao Ye (UoR)**

Copyright : **Water_Vapour_cci Consortium and ESA**

Document Change Log

Issue/ Revision	Date	Comment
1.0	13 August 2020	Issue 1 at end of Phase 2
1.1	13 October 2020	Updated according to RIDs on v1.0
2.0	7 June 2022	Issue 2 at end of Phase 3

TABLE OF CONTENTS

1. INTRODUCTION	7
1.1 Purpose.....	7
1.2 Structure of the document.....	7
2. ALGORITHM DEFINITION CDR-3	8
2.1 Introduction	8
2.2 Heritage.....	8
2.3 SPARC Data Initiative climatology construction	8
2.4 CDR-3 merging algorithm	9
2.5 Assumptions and limitations	12
3. ALGORITHM DEFINITION CDR-4	13
3.1 Introduction	13
3.2 Bias-correction on water vapour profiles	13
3.3 CDR-4 merging algorithm	17
3.4 Assumptions and limitations	18
4. SUMMARY AND CONCLUSIONS.....	20
APPENDIX 1: REFERENCES.....	21
APPENDIX 2: GLOSSARY	23

INDEX OF FIGURES

Figure 2-1: Example of SPARC Data Initiative climatology variables. The example shown here is for MIPAS April 2008.	9
Figure 2-2: Steps involved in the merging algorithm of CDR-3. (a) The water vapour time series of the different instruments are given in colours (see legend), the CCM in grey. (b) Instrumental differences to the CCM, here CMAM is used. (c) Bias-corrected instrument offsets. (d) Bias-corrected instrument time series and final merged dataset (black line with red diamonds) transferred back to the instrumental reference (average of Aura-MLS, ACE-FTS, and MIPAS).	11
Figure 3-1: Comparison of water vapour vertical profiles relative to thermal tropopause height from different satellite instruments and in-situ observations. The satellite observations are from the period 2010 to 2012, and the JULIA and FPH/CFH data from the period 2000 to 2016. From top to bottom: DJF, MAM, JJA and SON. From left to right: 90°S–60°S, 60°S–30°S, 30°S–30°N, 30°N–60°N, and 60°N–90°N. The water vapour mixing ratio is calculated for each 1 km altitude bin from -6 to +6 km range, with the mid-points of the altitude grid boxes at -5.5, -4.5, -3.5,..., +5.5 km, respectively. The grey and green shadings show the mean absolute deviation (MAD) of the mean mixing ratio from JULIA (black) and FPH/CFH (green), respectively.....	15
Figure 3-2: Example for the bias-correction method with the quantile-mapping technique with the MLS measurements.....	16
Figure 3-3: Merged VRWV monthly product at 250 hPa for July 2010.....	18

1. INTRODUCTION

1.1 Purpose

This document presents the final version of the algorithm theoretical baseline document (ATBD) for the merged VRWV CDR-3 v3.3 and CDR-4 v3.0 products as produced within Phase 1 of the ESA Water_Vapour_cci project. The purpose of the ATBD is to provide detailed information on the physical, mathematical and functional descriptions used in the merging algorithms for the two products and also their input datasets.

1.2 Structure of the document

This ATBD is structured as follows:

- Algorithm definition for CDR-3 and SPARC Data Initiative climatology input fields (Section 2)
- Algorithm definition for CDR-4 (Section 3)
- Summary and Conclusions (Section 4).

2. ALGORITHM DEFINITION CDR-3

2.1 Introduction

The ESA WV_cci CDR-3 features a long-term zonal monthly mean dataset of vertically resolved water vapour (VRWV) that consists of a merger between the satellite limb sounders SAGE II, UARS-MLS, HALOE, POAM III, SMR, SAGE III, SCIAMACHY, MIPAS, ACE-FTS, ACE-MAESTRO, Aura-MLS and SAGE III/ISS. A main goal of the construction of this CDR was the focus on correcting for spatio-temporal sampling differences and biases between input datasets.

2.2 Heritage

The methodological approach that has been used as basis for the WV_cci CDR-3 merging algorithm had been developed by Hegglin et al. (2014) [RD-1]. This merging method uses the stratospheric water vapour fields of a chemistry–climate model nudged to observed meteorology as a transfer function between different satellite instruments. This approach has been shown to overcome issues arising from short overlap periods and instrument drifts, which are more likely towards the end of mission lifetimes when satellite instruments can suffer degradation and satellite orbits start to drift.

2.3 SPARC Data Initiative climatology construction

As input data to CDR-3, the SPARC Data Initiative monthly zonal mean climatologies are being used. More instrument-specific information on these input datasets can be found in SPARC (2017) [RD-2], Hegglin et al. (2013) [RD-3], and Hegglin et al. (2021) [RD-4], but we here give a short general summary of how the climatologies are constructed.

Monthly zonal mean time series of water vapour have been calculated for fields on the SPARC Data Initiative climatology grid, using 5° latitude bins (with mid-points at -87.5°, -82.5°, -77.5°, ..., 87.5°) and 28 pressure levels (300, 250, 200, 170, 150, 130, 115, 100, 90, 80, 70, 50, 30, 20, 15, 10, 7, 5, 3, 2, 1.5, 1, 0.7, 0.5, 0.3, 0.2, 0.15 and 0.1 hPa). Water vapour is reported as volume mixing ratios (VMR) along with the 1- σ standard deviation, the number of averaged data values given for each month, latitude bin, and pressure level. In addition, the mean, minimum, and maximum local solar time (LST), average day of the month, and average latitude of the data within each bin for one selected pressure level are also provided (see Figure 2-1).

Original data have been carefully screened according to recommendations given in relevant quality documents, in the published literature, or according to the best knowledge of the involved instrument scientists. Monthly zonal mean products are calculated as the average of all of the measurements on a given pressure level within each latitude bin and month. An exception is MIPAS, for which measurements are interpolated to the centre of the latitude bin after averaging. For some instruments, averaging was done in $\log_{10}(\text{VMR})$ space. If not otherwise mentioned, a minimum of five measurements within the bin is required to calculate a monthly zonal mean for each instrument.

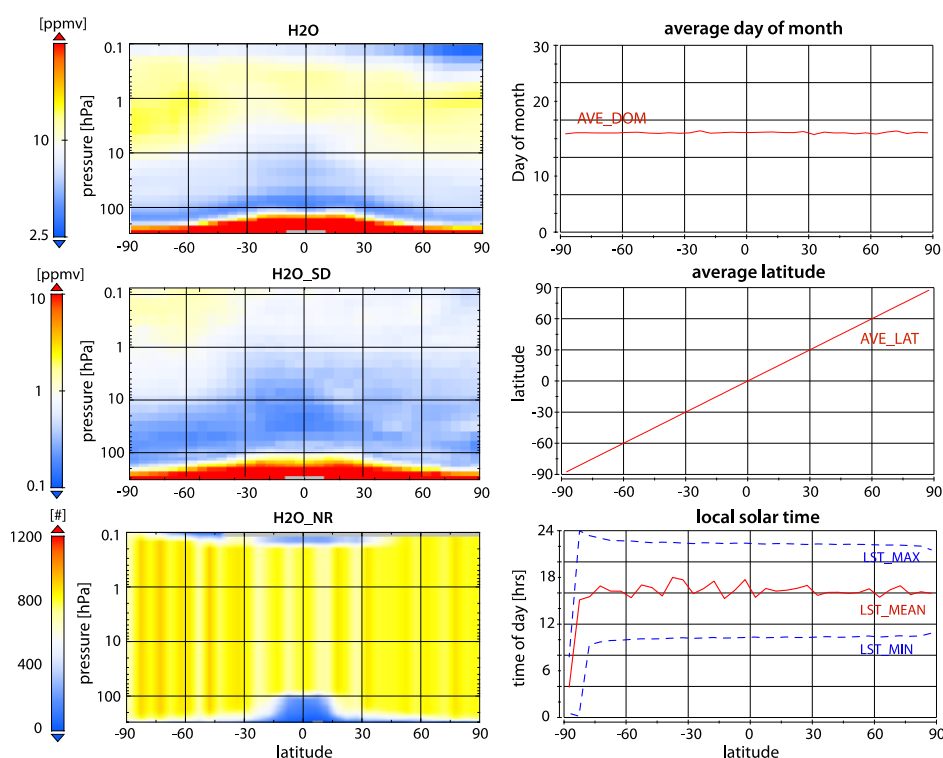


Figure 2-1: Example of SPARC Data Initiative climatology variables. The example shown here is for MIPAS April 2008.

2.4 CDR-3 merging algorithm

The merging algorithm is described in detail in Hegglin et al. (2014) [RD-1] and summarised here. It consists of the following steps that are also exemplified in Figure 2-2:

- The monthly zonal mean SPARC Data Initiative data of the individual instruments described in Section 2.3, are used as input to the merging algorithm.

- For each instrument (i), latitude grid, and pressure level, a mean offset between the observed and modelled water vapour time series is calculated as an average over the full mission (i.e. without time-dependency) according to

$$d[H_2O]_i = \langle [H_2O]_i \rangle - \langle [H_2O]_{CCM} \rangle \quad (\text{Equation 1})$$

where i denotes a given instrument and CCM a chemistry–climate model nudged to observed meteorology.

- In a second step, each time series is bias-corrected with respect to a reference (here calculated as the average of Aura-MLS, MIPAS, and ACE-FTS) using the biases calculated according to Equation 1 for both instrument i and reference Ref . The resulting bias-corrected water vapour concentration for each instrument ($[H_2O]_{i_{bc}}$) can thereby be expressed as:

$$[H_2O]_{i_{bc}} = [H_2O]_i - d[H_2O]_i + d[H_2O]_{Ref} \quad (\text{Equation 2})$$

- In a third step, the bias-corrected water vapour time series are being scanned for unphysical values (that is negative values), detected outliers are filtered out, and the remaining data points are merged to a bias-corrected monthly mean using an optimal estimation approach to merge the multi-instrument data points (MIM_{bc}):

$$[H_2O]_{MIM_{bc}} = \sum_{i=1}^N \alpha_i [H_2O]_{i_{bc}} (\sum_{i=1}^N \alpha_i)^{-1} \quad (\text{Equation 3})$$

where N denotes the number of instruments available, and α_i is the weighting factor for each instrument. Currently, α_i is calculated as the moment of each instrument's bias-corrected differences (seen in Figure 2-2, panel c).

As shown in Figure 2-2, the biases between the individual instrument time series have been removed after step 2.

Each step in the procedure has gone through visual inspection so to ensure correct functioning of the merging algorithm, which has been continuously automated. The implementation of an optimal estimation approach for the merging is the most innovative improvement of the merging methodology put forward by Hegglin et al. (2014) [RD-1] and provides a first essential step towards dealing with inconsistent seasonal cycle amplitudes, outliers, and sampling issues that may affect anomalies. However, these points will need further investigation as planned for WV_cci Phase 2.

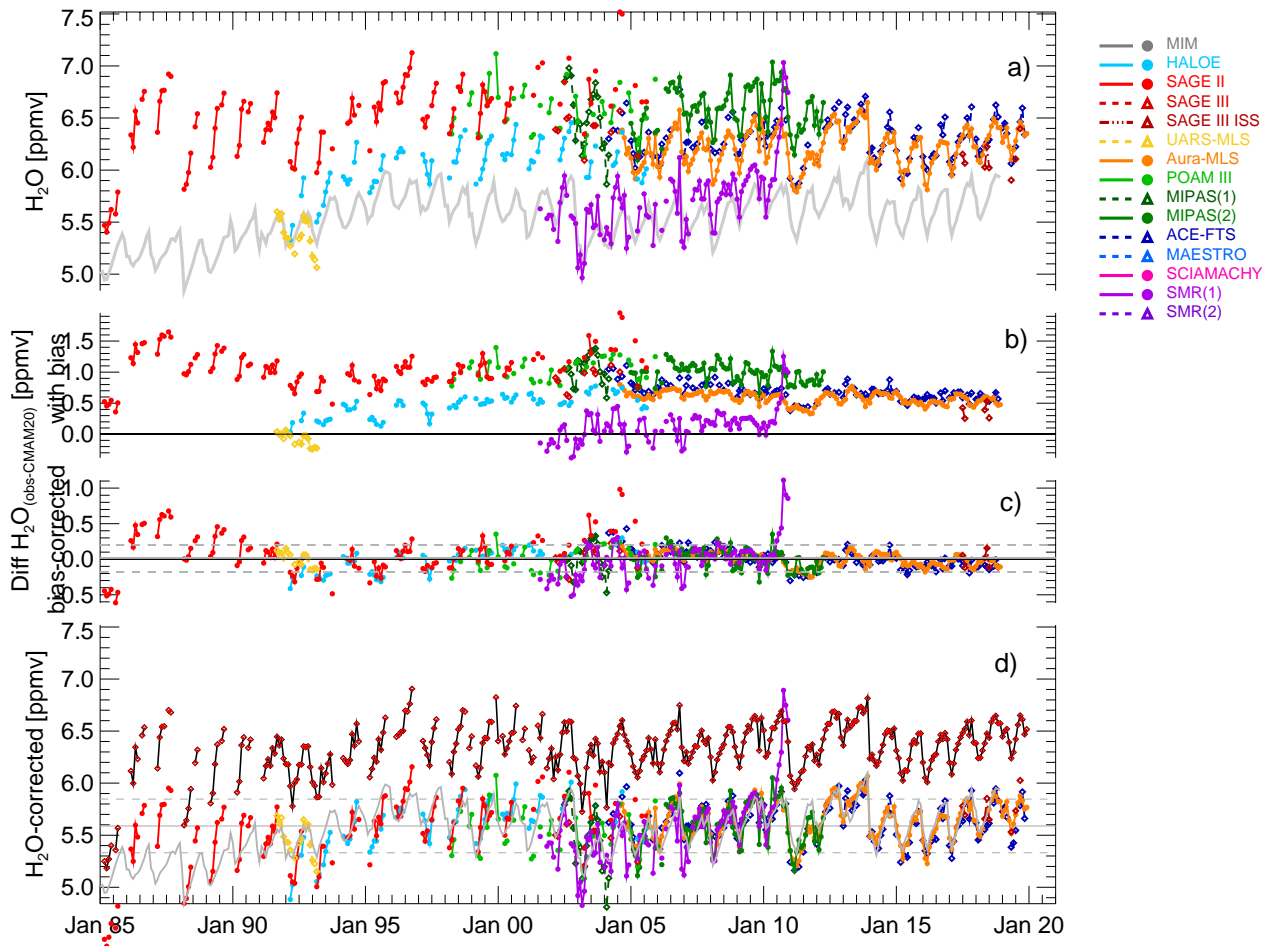


Figure 2-2: Steps involved in the merging algorithm of CDR-3. (a) The water vapour time series of the different instruments are given in colours (see legend), the CCM in grey. (b) Instrumental differences to the CCM, here CMAM is used. (c) Bias-corrected instrument offsets. (d) Bias-corrected instrument time series and final merged dataset (black line with red diamonds) transferred back to the instrumental reference (average of Aura-MLS, ACE-FTS, and MIPAS).

2.5 Assumptions and limitations

The main assumption underlying the merging methodology is that the quality of the chemistry–climate model simulation is sufficient so as not to introduce spurious trends into the merged observational time series. This seems justified, since all the transfer function does is to shift a given instrument record by an absolute amount and does not affect the time series evolution in any other way. We have so far used the Canadian Middle Atmosphere Model CMAM as transfer function, since its stratospheric transport has been tested rigorously and its representation of other trace gases has been shown to be promising (e.g. Shepherd et al., 2014 [RD-5]). This assumption will, however, need to be further tested in WV_cci Phase 2 by using different models as transfer function that are known to show somewhat different behaviour (e.g. Lossow et al., 2018 [RD-6]).

The implementation of the optimal estimation approach in the final merging step is new and will need further testing. In particular, the choice of using the mean bias-corrected differences as weighting in the optimal estimation equation, which again are potentially too dependent on the model behaviour, could be replaced with different approaches. This potential limitation will be investigated further in WV_cci Phase 2.

3. ALGORITHM DEFINITION CDR-4

3.1 Introduction

The objective of ESA WV_cci CDR-4 is to construct a prototype three-dimensional vertically resolved water vapour dataset in the upper troposphere and lower stratosphere (UTLS) region by merging both limb- and nadir-viewing satellite observations from Aura-MLS, MIPAS and IMS. The nadir-viewing geometry delivers reliable VRWV profiles with high precision mainly in the troposphere and the limb-viewing geometry mainly covers VRWV profiles in the stratosphere and above. In the UTLS region, due to the very strong vertical gradients in water vapour concentrations, both types of viewing geometries lead to large uncertainties. The merged prototype product CDR-4 takes advantages from these two types of viewing geometry to improve the quality of the VRWV profile data in this region.

The methodology to be used for the merging of observations from the two viewing geometries is based on the bias-correction relative to the *in situ* VRWV profiles from balloon-borne hygrometer (BBH, same as FPH/CFH) observations. All the input data will be bias-corrected via a quantile-mapping technique (Maraun, 2013 [RD-7]) and turned into a harmonised limb/nadir data record of VRWV in the UTLS region. These harmonised VRWV data from multiple satellite instruments are then merged into a three-dimensional VRWV product CDR-4.

3.2 Bias-correction on water vapour profiles

The original retrieved water vapour profiles consist of limb measurements from Aura-MLS and MIPAS instruments and the nadir data product IMS (which is based on a combination of IASI, MHS and AMSU satellite measurements). As mentioned in Section 3.1, the input VRWV profiles from different satellite instruments will be bias-corrected via a quantile-mapping technique in comparison to reference data from BBH observations. Limited to the spatial and temporal coverage of the BBH observations, the comparisons are performed in a common geophysical reference coordinate system – here, the thermal tropopause height is chosen – to reduce geophysical noise.

Figure 3-1 shows the comparison of VRWV profiles from different satellites to reference datasets in a geophysical-based vertical coordinate system (here, using the thermal tropopause as reference). Due to limited spatial and temporal coverage, JULIA aircraft data is not used in the bias-correction process and only BBH profile observations are chosen as

reference data (see DARD [RD-8]). The comparisons to BBH profile data clearly show that the limb WV data match well with hygrometer profiles above the tropopause and the nadir VRWV data from IMS agree better with the hygrometer profiles below the tropopause. Due to the limitation of the spatial and temporal coverage, the highly sparse ACE-FTS and ACE-MAESTRO are not included in the production of CDR-4 data.

In Figure 3-1, all profiles from satellites and BBH are screened with quality control suggestions from each instrument. It is noteworthy to mention that the comparison is carried out in five latitude bands: 90°S–60°S, 60°S–30°S, 30°S–30°N, 30°N–60°N, and 60°N–90°N, due to the limitation of the sparse BBH observations. The following bias-correction process will also be performed in each latitude band. As there is no BBH site in the latitude band 90°S–60°S, the original profiles from all satellite observations are used in the production of CDR-4 data in this band. The choice of these latitude bands leads to the problem with tropospheric/stratospheric intrusions around 30° in latitude, in the case of double thermal tropopause. In practice, only the lowest thermal tropopause is used in this study and the tropopause height of 14 km is chosen as the limit to deal with tropospheric/stratospheric intrusions. The tropical profiles (30°S–30°N) with a tropopause height less than 14 km are treated as stratospheric intrusions from mid-latitude and assigned into mid-latitude bands. Conversely, the mid-latitude profiles with a tropopause height larger than 14 km are regarded as tropospheric intrusions from tropical regions and assigned into the tropical band. This latitude correction on the profiles leads to a remarkable reduction of variation within the mean water vapour profiles in the tropopause-based coordinate.

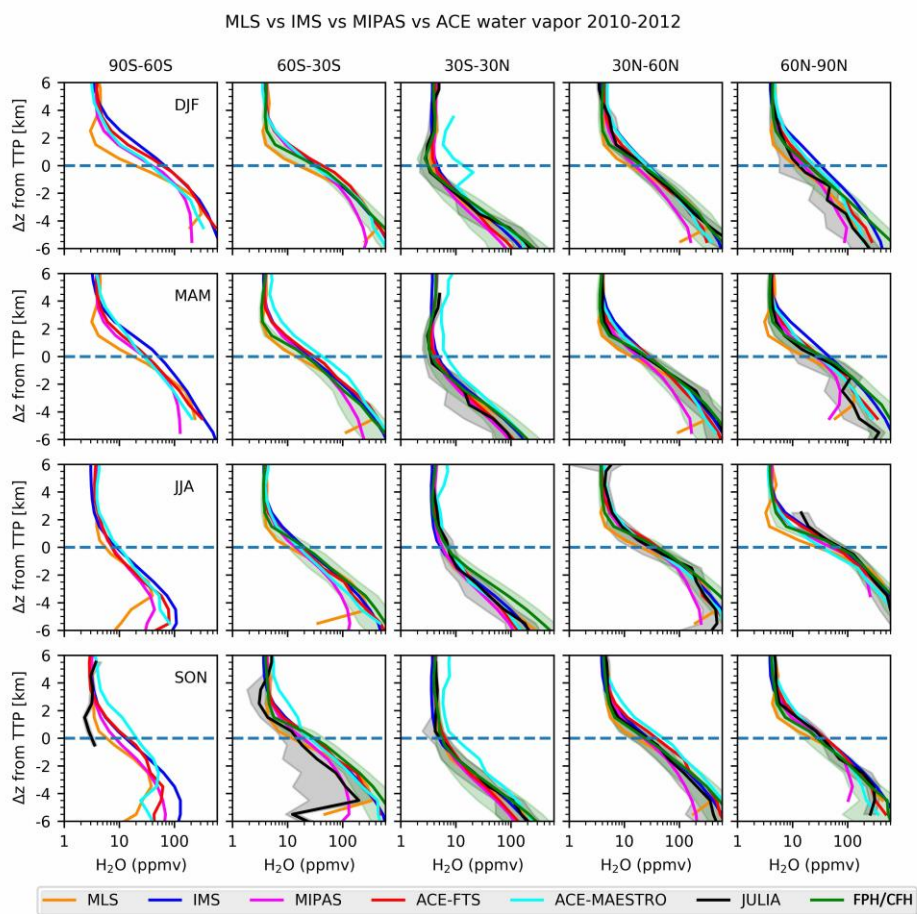


Figure 3-1: Comparison of water vapour vertical profiles relative to thermal tropopause height from different satellite instruments and in-situ observations. The satellite observations are from the period 2010 to 2012, and the JULIA and FPH/CFH data from the period 2000 to 2016. From top to bottom: DJF, MAM, JJA and SON. From left to right: 90°S–60°S, 60°S–30°S, 30°S–30°N, 30°N–60°N, and 60°N–90°N. The water vapour mixing ratio is calculated for each 1 km altitude bin from -6 to +6 km range, with the mid-points of the altitude grid boxes at -5.5, -4.5, -3.5, ..., +5.5 km, respectively. The grey and green shadings show the mean absolute deviation (MAD) of the mean mixing ratio from JULIA (black) and FPH/CFH (green), respectively.

The bias-correction algorithm is applied to VRWV profiles from each satellite instrument in the tropopause-based vertical coordinate. For each month and latitude band (see Figure 3-1), the VRWV biases between each satellite instrument and BBH observations are calculated using a quantile-mapping technique for each 1 km altitude bin within the -6 to +6 km range. For each altitude bin in each month, the biases are computed through the cumulative distribution function (CDF) for the WV measurements as:

$$WV_{k,corrected} = F_{GRUAN}^{-1}[F_k(WV_k)], \tag{Equation 4}$$

where the F_{GRUAN}^{-1} is the inverse CDF for BBH observations and F_k is the CDF for the input data from each satellite instrument. Note that the WV_k here is taken as the logarithm of the mixing ratio. As the quantile-mapping technique uses the quantile–quantile matching to converge the satellite WV distribution function to the BBH one, the biases between WV profiles from each satellite instrument and BBH observations are calculated for each quantile. These biases are applied back to the original satellite VRWV profiles on the original vertical levels. Figure 3-2 shows an example of the distribution of bias-corrected WV measurements from MLS in the range 2–3 km below the tropopause in the tropical region. It indicates that the bias-corrected WV from each satellite instrument has a much better agreement with the BBH observations. As mentioned above, in the latitude range 90S–60S, the bias-correction is not available due to lack of BBH observations. Note, this will introduce a discontinuity in the dataset and an associated increase in measurement uncertainty.

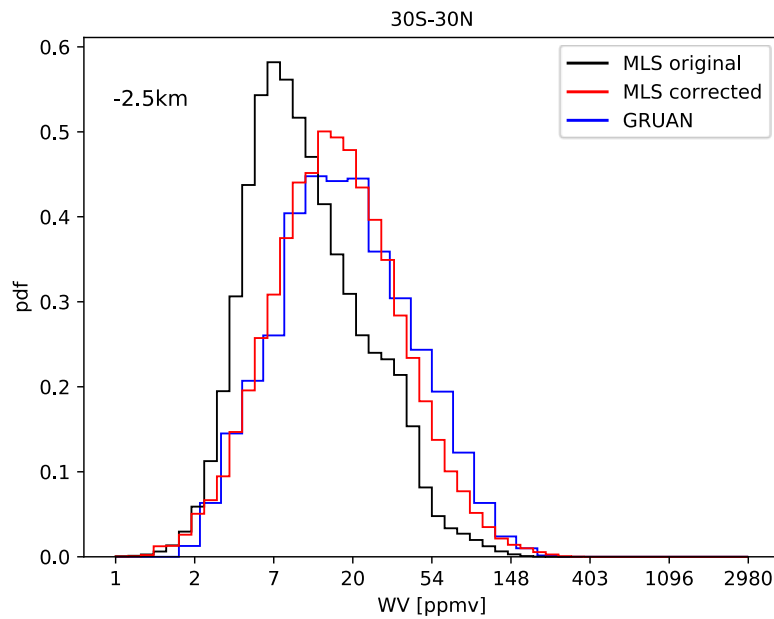


Figure 3-2: Example for the bias-correction method with the quantile-mapping technique with the MLS measurements.

For creating monthly mean data for the individual instruments, the bias-corrected VRWV profiles are taken for a temporal and spatial level 3 aggregation. The aggregation is performed for each month in 2010–2012 with a horizontal resolution of 5 degrees by 5 degrees in latitude and longitude. In the vertical dimension, the L2 VRWV profiles are interpolated to 26 pressure levels from 1000 hPa up to 10 hPa (1000, 950, 900, 850, 800, 750, 700, 650, 600, 550, 500, 450, 400, 350, 300, 250, 225, 200, 175, 150, 125, 100, 70, 50,

30, 10 hPa), as also specified in the PSD [RD-9]. For all sensors, the monthly average is computed as the mean of VRWV profiles $q_k(x, y, z)$:

$$q(x, y, z) = \frac{1}{N} \sum q_k(x, y, z), \quad (\text{Equation 5})$$

where N is the number of measurements. Note that for IMS, the average VRWV is calculated based on the logarithm of mixing ratio, same as the original VRWV profiles. The uncertainty of the monthly mean σ_q can be estimated as the standard error of the mean:

$$\sigma_q(x, y, z) = \sqrt{S^2(x, y, z)/N}, \quad (\text{Equation 6})$$

where $S^2(x, y, z)$ is the variance of the WV measurements calculated as:

$$S^2(x, y, z) = \frac{1}{N-1} \sum [q_k(x, y, z) - q(x, y, z)]^2. \quad (\text{Equation 7})$$

3.3 CDR-4 merging algorithm

The merged monthly mean dataset of VRWV profiles is created from several satellite instruments: limb VRWV data from Aura-MLS and MIPAS and nadir VRWV data from RAL IMS. The monthly mean data from individual instruments, which are described in Section 3.2, are here used to calculate the merged monthly mean VRWV CDR-4. Due to the limited spatial coverage of BBH observations, the merged product consists of a combination of original VRWV and bias-corrected VRWV profiles at different pressure levels following the merging rules given below:

- at and above 100 hPa (lower stratosphere), only original VRWV monthly mean data from MLS and MIPAS before bias-correction are used to calculate the average;
- between 100 hPa and 300 hPa, the bias-corrected VRWV monthly mean data of all instruments are used to calculate the average;
- below 300 hPa (troposphere), only original VRWV monthly mean data from IMS before bias-correction are used to calculate the average.

In the lower stratosphere, the amount of BBH observations is not enough for a reliable bias-correction to the limb satellite observations and the original limb WV has a relatively high accuracy, thus the bias-corrected data are not included in the merged product. In the troposphere, the original nadir VRWV profiles retrieved from IMS also show very high

accuracy and only the original month mean data are used in the merged product. An example of the merged VRWV CDR-4 product is shown in Figure 3-3.

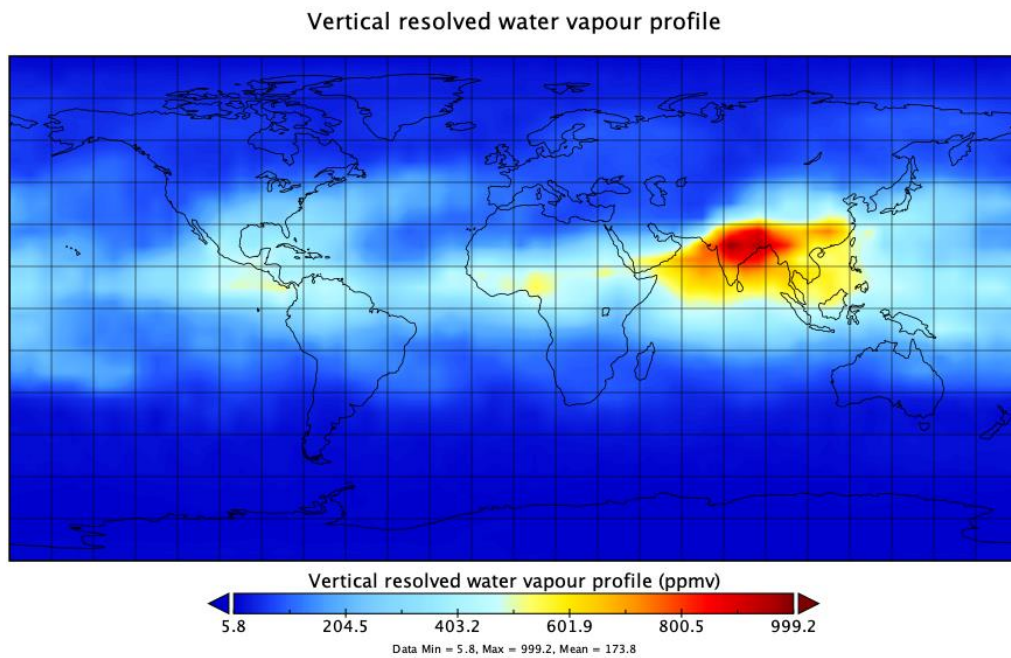


Figure 3-3: Merged VRWV monthly product at 250 hPa for July 2010.

All data are included in one NetCDF4 file, which includes the merged data and the corresponding uncertainty for each grid point.

3.4 Assumptions and limitations

The main assumption in the algorithm to construct the VRWV CDR-4 product in the UTLS region is that VRWV profiles from BBH observations are representative for the bias-correction applied to the VRWV data from satellite instruments. Due to the limited spatial and temporal coverage of the BBH observations, a bias-correction of the VRWV profile data based on a validation with coincident BBH observations is not feasible. Instead, the tropopause height, a meteorological feature that determines the structure found in UTLS water vapour [RD-10–RD-14], is chosen as the geophysical reference coordinate system in the vertical. In this new tropopause-based coordinate system, the biases in VRWV can be calculated between satellite instruments, and BBH observations including VRWV data obtained over a larger geographical domain. With the bias-correction applied to the VRWV data from satellite instruments, it is possible to merge together the VRWV profiles from both limb- and nadir-viewing geometries into a single data product. It is highlighted here that the merging approach is assumed to mostly correct for the smoothing characteristics of the averaging kernels of the respective instruments.

For this prototype CDR-4 product, there are still several limitations:

1. Biases between satellite data and BBH observations in the geophysical reference coordinate system are calculated within several broad latitude bands, thus the longitudinal variations of these biases may not be fully accounted for in this process. It should also be noted that in latitude bands where no BBH observations are available, the lack of a bias-correction may currently lead to discontinuities between adjacent latitude bands. Tests on the bias-correction algorithm with ERAi reanalysis WV data show that the spatial and temporal coverage of the reference data have a notable impact on the quality of bias-correction to the satellite profiles. Thus, more frequent and denser BBH observations (or an alternative instrument reference) are needed across the globe for a quantitatively better bias-correction for the satellite observations.
2. The satellite instruments show a big difference in the amount of VRWV profile measurements across the UTLS. The proportional contribution of each satellite observations to the merged CDR-4 product is important to the final data quality. An appropriate weighting scheme to the satellite data based on the derived input quality and derived instrument-dependent biases is essential for improving the final product quality.
3. The merging rules are likely to bring in a discontinuity in the merged CDR-4 product at 300 and 100 hPa. Assessment of this merging problem shows that there is no need for post-processing at 100 hPa due to the high quality of instrument WV values and variations. Meanwhile, a smoothing process is applied to VRWV profiles across the 300-hPa level for IMS based on a window function, here using the Blackman window. The smooth processing reduces the sharp discontinuity at 300 hPa between original and bias-correction profiles. To obtain a harmonised and continuous WV data in the vertical, the bias-correction for and merging process of satellite VRWV profiles should be performed throughout the UTLS and troposphere in the future.

4. SUMMARY AND CONCLUSIONS

For CDR-3, the merging algorithm by Hegglin et al. (2014) [RD-1] has been further developed towards operational implementation. Several refinements have been applied, in particular, the optimal estimation theory as new approach for the merging of the different satellite instrument inputs. While this merging approach addresses many instrumental issues identified as potential problems in the merging process, others still need further implementation and will be the focus of the continued improvements of CDR-3 in WV_cci Phase 2. However, the final quality of the dataset is limited mainly by the temporal and spatial coverage of the limb satellite input data, especially in the early years of the instrumental record as is detailed in the PVIR [RD-15].

For CDR-4, a new prototype merging algorithm is under development that applies a novel bias-correction methodology (quantile mapping) to the input profiles before merging. This methodology accounts for biases in the limb and nadir satellite sounders across the UTLS region, including the smoothing resulting from averaging kernels that are too broad to resolve the vertical gradients found in WV across this region. While the merging algorithm has been found to be promising, limitations arise from a too-scarce spatio-temporal coverage in the reference datasets used for the bias-correction (BBH observation stations).

APPENDIX 1: REFERENCES

- RD-1. Hegglin, M. I., D. Plummer, J. Scinocca, T. G. Shepherd, J. Anderson, L. Froidevaux, B. Funke, D. Hurst, A. Rozanov, J. Urban, T. v. Clarmann, K. A. Walker, R. Wang, S. Tegtmeier, and K. Weigel, Variation of stratospheric water vapour trends with altitude from merged satellite data, *Nature Geoscience*, doi: 10.1038/NGEO2236, 2014.
- RD-2. SPARC, 2017: The SPARC Data Initiative: Assessment of stratospheric trace gas and aerosol climatologies from satellite limb sounders. By M. I. Hegglin and S. Tegtmeier (eds.), *SPARC Report No. 8*, WCRP-5/2017, doi:10.3929/ethz-a-010863911.
- RD-3. Hegglin, M.I., Tegtmeier, S., Anderson, J., Froidevaux, L., Fuller, R., Funke, B., Jones, A., Lingenfelter, G., Lumpe, J., Pendlebury, D. and Remsberg, E., SPARC Data Initiative: Comparison of water vapor climatologies from international satellite limb sounders. *J. Geophys. Res.: Atmospheres*, 118(20), pp.11-82, 2013.
- RD-4. Hegglin, M. I., Tegtmeier, S., Anderson, J., Bourassa, A. E., Brohede, S., Degenstein, D., Froidevaux, L., Funke, B., Gille, J., Kasai, Y., Kyrölä, E. T., Lumpe, J., Murtagh, D., Neu, J. L., Pérot, K., Remsberg, E. E., Rozanov, A., Toohey, M., Urban, J., von Clarmann, T., Walker, K. A., Wang, H.-J., Arosio, C., Damadeo, R., Fuller, R. A., Lingenfelter, G., McLinden, C., Pendlebury, D., Roth, C., Ryan, N. J., Sioris, C., Smith, L., and Weigel, K.: Overview and update of the SPARC Data Initiative: comparison of stratospheric composition measurements from satellite limb sounders, *Earth Syst. Sci. Data*, 13, 1855–1903, <https://doi.org/10.5194/essd-13-1855-2021>, 2021.
- RD-5. Shepherd, T.G., Plummer, D.A., Scinocca, J.F., Hegglin, M.I., Fioletov, V.E., Reader, M.C., Remsberg, E., Von Clarmann, T. and Wang, H.J., Reconciliation of halogen-induced ozone loss with the total-column ozone record. *Nature Geoscience*, 7(6), pp.443-449, 2014.
- RD-6. Lossow, S., Hurst, D. F., Rosenlof, K. H., Stiller, G. P., von Clarmann, T., Brinkop, S., Dameris, M., Jöckel, P., Kinnison, D. E., Plieninger, J., Plummer, D. A., Ploeger, F., Read, W. G., Remsberg, E. E., Russell, J. M., and Tao, M.: Trend differences in lower stratospheric water vapour between Boulder and the zonal mean and their role in understanding fundamental observational discrepancies, *Atmos. Chem. Phys.*, 18, 8331–8351, <https://doi.org/10.5194/acp-18-8331-2018>, 2018.
- RD-7. Maraun, D., 2013: Bias Correction, Quantile Mapping, and Downscaling: Revisiting the Inflation Issue. *J. Climate*, 26, 2137–2143, <https://doi.org/10.1175/JCLI-D-12-00821.1>.
- RD-8. ESA CCI Water Vapour: Data Access Requirement Document. M. Schröder, M. Hegglin, H. Brogniez, J. Fischer, D. Hubert, A. Laeng, R. Siddans, C. Sioris, G. Stiller, T. Trent, K. Walker, O. Danne, U. Falk and H. Ye. Issue 3.2, 27 July 2021.

- RD-9. ESA CCI Water Vapour: Product Specification Document. M. Schröder, M. Hegglin, O. Danne, J. Fischer, A. Laeng, R. Siddans, C. Sioris, G. Stiller and K. Walker. Issue 3.2, 27 July 2021.
- RD-10. Hoor, P., C. Gurk, D. Brunner, M. I. Hegglin, H. Wernli, and H. Fischer (2004): Seasonality and extent of extratropical TST derived from in-situ CO measurements during SPURT, *Atmos. Chem. Phys.*, 4, 1427–1442.
- RD-11. Hegglin, M. I., D. Brunner, Th. Peter, P. Hoor, H. Fischer, J. Staehelin, M. Krebsbach, C. Schiller, U. Parchatka, and U. Weers (2006): Measurements of NO, NO_y, N₂O, and O₃ during SPURT: Implications for transport and chemistry in the lowermost stratosphere, *Atmos. Chem. Phys.*, 6, 1331-1350.
- RD-12. Hegglin, M. I., C. D. Boone, G. L. Manney, T. G. Shepherd, K. A. Walker, P. F. Bernath, W. H. Daffer, P. Hoor, and C. Schiller (2008): Validation of ACE-FTS satellite data in the upper troposphere/lower stratosphere (UTLS) using non-coincident measurements, *Atmos. Chem. Phys.*, 8, 1483–1499.
- RD-13. Hegglin, M. I., C. D. Boone, G. L. Manney, and K. A. Walker (2009): A global view of the extratropical tropopause transition layer (ExTL) from Atmospheric Chemistry Experiment Fourier Transform Spectrometer O₃, H₂O, and CO, *J. Geophys. Res.*, 114, D00B11, doi: 10.1029/2008JD009984.
- RD-14. Schwartz, M. J., G. L. Manney, M. I. Hegglin, N. J. Livesey, M. L. Santee, W. H. Daffer, Climatology and variability of trace gases in extratropical double-tropopause regions from MLS, HIRDLS, and ACE-FTS measurements, *J. Geophys. Res. Atmos.*, 120, doi:10.1002/2014JD021964, 2015.
- RD-15. ESA CCI Water Vapour: Product Validation and Intercomparison Report, Part 2. H. Ye, M. Hegglin, M. Schröder, A. Niedorf. Issue 2.0, 1 June 2022.

APPENDIX 2: GLOSSARY

Term	Definition
<i>ATBD</i>	Algorithm Theoretical Basis Document
<i>BBH</i>	Balloon-borne Hygrometer
<i>CCI</i>	ESA Climate Change Initiative
<i>CDF</i>	Cumulative Distribution Function
<i>DARD</i>	Data Access Requirement Document
<i>E3UB</i>	End to End ECV Uncertainty Budget
<i>ESA</i>	European Space Agency
<i>IMS</i>	Infra-red Microwave Sounder scheme
<i>PVIR</i>	Product Validation and Intercomparison Report
<i>UTLS</i>	Upper troposphere and lower stratosphere
<i>VRWV</i>	Vertical Resolved Water Vapour

End of Document